International Journal of Electrical, Electronic and Communication Sciences
ISSN: 2517-9438
Vol:10, No:11, 2016

Applicability of Linearized Model of Synchronous Generator for Power System Stability Analysis

J. Ritonja, B. Grcar

***Abstract*—**For the synchronous generator simulation and analysis and for the power system stabilizer design and synthesis a mathematical model of synchronous generator is needed. The model has to accurately describe dynamics of oscillations, while at the same time has to be transparent enough for an analysis and sufficiently simplified for design of control system. To study the oscillations of the synchronous generator against to the rest of the power system, the model of the synchronous machine connected to an infinite bus through a transmission line having resistance and inductance is needed. In this paper, the linearized reduced order dynamic model of the synchronous generator connected to the infinite bus is presented and analysed in details. This model accurately describes dynamics of the synchronous generator only in a small vicinity of an equilibrium state. With the digression from the selected equilibrium point the accuracy of this model is decreasing considerably. In this paper, the equations' descriptions and the parameters' determinations for the linearized reduced order mathematical model of the synchronous generator are explained and summarized and represent the useful origin for works in the areas of synchronous generators' dynamic behaviour analysis and synchronous generator's control systems design and synthesis. The main contribution of this paper represents the detailed analysis of the accuracy of the linearized reduced order dynamic model in the entire synchronous generator's operating range. Borders of the areas where the linearized reduced order mathematical model represents accurate description of the synchronous generator's dynamics are determined with the systemic numerical analysis. The thorough eigenvalue analysis of the linearized models in the entire operating range is performed. In the paper, the parameters of the linearized reduced order dynamic model of the laboratory salient poles synchronous generator were determined and used for the analysis. The theoretical conclusions were confirmed with the agreement of experimental and simulation results.

***Keywords*—**Eigenvalue analysis, mathematical model, power system stability, synchronous generator.

I. Introduction

THE synchronous generators (SG) are most important sources of electric energy. Consequently, there is a distinct interest in adequate static and dynamic models of SG. These models accelerate the design and the construction of SG, facilitate the analysis and simulation of operating of SG and enable the systematic synthesis of their control systems.

In [1]-[3], an excess number of the SG's models of varying degrees of complexity are presented. The simplest SG's model is a "voltage behind synchronous reactance model" or a "classical model" where SG is represented with a network of constant voltage and single series reactance. On the other side, the most thorough SG's model is the "non-linear 7th order d-q model" (N7OM), where magnetic coupling of stator-, field- and damper- windings is a function of a position and saturation of a rotor. The windings' equations are transformed and presented in a form of a non-linear state-space model. Between these two extreme models, we can find many SG's models with a different grade of complexity. Especially important is the "linearized 3rd order model" (L3OM), called also "Heffron–Phillips model of synchronous generator" [4]. This model has a very good ratio between complexity and accuracy [2].

Limitations of utilization of L3OM are presented in its early literature [1], [4]. In that period, critical assessments of usage of L3OM are carried out. Numerous attempts of modification of L3OM toward its generalization and larger functionality are conducted. However, none of those attempts replaced an original version of L3OM.

In a majority of works concerned with the dynamics of SG, L3OM is used [1]-[5]. The main reason to use L3OM are its simple linear structure, which allows use of linear methods for a model analysis, and a small number of known SG's data necessary for calculation of model's coefficients.

Many authors assume the results of L3OM are similar enough with the results of full order N7OM (e.g. [6]). But L3OM assures accurate results only in relative proximity of an initial steady-state. N7OM is the superior one and that in general L3OM cannot replace N7OM. However, there are certain niches where L3OM seems adequate. A goal of the presented work is to explore applicability of L3OM involving certain operating areas and limits in where it can replace N7OM without significantly lacking accuracy.

In Sections II and III, N7OM and L3OM are presented in a unifying way displaying the complexity of the both models and the demand for the SG's data. Such description enables comparison of advantages and disadvantages of the both models and helps to select a proper model for case-by-case scenarios. In Section IV, studied SG and a testing system are described. Testing methods used for determination of the SG's data are listed. Measured SG's data and the calculated coefficients of the models are presented. Simulation results of the both models are compared with the experimental results of laboratory tested SG. Matching responses of L3OM and the experimental object is presented in two phases: first, N7OM with measured parameters is shown to be accurate enough for description of dynamics of the object. Second, such N7OM is used further as a reference model. This way enables quicker comparison of L3OM and the real object. In Section V, a detailed numerical analysis of L3OM is presented. The both

Assoc. Prof. Dr. Jozef Ritonja is with the University of Maribor, Slovenia (e-mail: jozef.ritonja@um.si).

models are compared in Section VI.

II. Non-Linear 7-th Order Model of SG

Considered SG is assumed to have three stator windings, one field winding and two damper windings, which are magnetically coupled. The SG is connected to a large power system with constant frequency and constant voltage (an infinite bus) through a transmission line. An original model represents six flux linkage equations with self- and mutual-stator and rotor inductances [1], [2]. This model is transformed by means of Park's matrix transformation into a model with orthogonal axes, i.e. the N7OM model. The machine equations are formulated in a state-space form. The model's inputs are mechanical torque $T_m(t)$ and rotor excitation winding voltage $v_f(t)$. The model's state-space variables are stator d-axis flux linkage $\lambda_d(t)$, stator q-axis flux linkage $\lambda_q(t)$, rotor excitation winding flux linkage $\lambda_F(t)$, rotor d-axis damper winding flux linkage $\lambda_D(t)$, rotor q-axis damper winding flux linkage $\lambda_D(t)$, mechanical rotor speed $\omega(t)$ and electric rotor angle $\delta(t)$.

The necessary parameters and steady-state quantities of SG to calculate the coefficients and initial conditions of N7OM are presented in Table I.

TABLE I
SG'S DATA FOR N7OM

Parameters of SG	L_d [H], L_q [H], L_d' [H], L_d'' [H], l_d [H], l_q [H], R_s [Ω], R_F [Ω], R_D [Ω], R_Q [Ω], R_e [Ω], L_e[H], H [s]
Steady-state quantities of SG	P [W], Q [VAr], ω_s [rad s^{-1}], V_∞ [V]

The parameters in Table I: L_d and L_q are d- and q-axes inductances; L_d' and L_d'' are d-axis transient and sub-transient inductances; l_d and l_q are d- and q-axes leakage inductances; R_F, R_D, R_Q are stator-, field-, d-axis damping- and q-axis damping- windings resistances; H is an inertia constant; R_e and L_e are transmission line resistance and reactance, respectively. The steady-state quantities in Table I: P and Q are active and reactive power at a machine terminal; ω_s is electric synchronous speed and V_∞ is infinite bus voltage.

All the determined parameters and symbols must be normalized on base quantities. To convert dimensional to normalized quantities and conversely, the base quantities presented in Table II are required.

TABLE II
SG'S BASE QUANTITIES

Primary base quantities	$S_{base,1p}$ [VA], $V_{base,L0}$ [V], ω_{base} [rad s^{-1}],
Secondary stator base quantities	I_{base} [A], R_{base} [Ω], L_{base} [H]
Quantity for conversion between stator and rotor base quantities	I_{F0} [A]
Field and damping base quantities	I_{Fbase} [A], V_{Fbase} [V], R_{Fbase} [Ω], L_{Fbase} [H], R_{Dbase} [Ω],L_{Dbase} [H], R_{Qbase} [Ω], L_{Qbase} [H]

Meaning of symbols in Table II: $S_{base,1p}$ is stator base power, which is equal to rated one-phase apparent power; $V_{base,L0}$ is stator base voltage, which is equal to an effective stator rated line to neutral voltage; ω_{base} is equal to electric synchronous speed; I_{base}, R_{base} and L_{base} are calculated stator base current, resistant and inductance, respectively; I_{F0} is field current corresponding to the rated stator voltage on an air gap line; I_{Fbase}, V_{Fbase}, R_{Fbase}, L_{Fbase}, R_{Dbase}, L_{Dbase}, R_{Qbase} and L_{Qbase} are field and damping current, voltage, resistance and inductance base quantities.

For N7OM, all the SG's parameters and variables must be normalized by means of the presented base values. The inputs and state-space variables of N7OM are collected in Table III. All inputs and variables except an electric rotor angle are normalized.

TABLE III
N7OM'S INPUTS AND STATE-SPACE VARIABLES

Inputs of N7OM	$T_m(t)$, $v_f(t)$
State-space variables of N7OM	$\lambda_d(t)$, $\lambda_q(t)$, $\lambda_F(t)$, $\lambda_D(t)$, $\lambda_Q(t)$, $\omega(t)$, $\delta(t)$

For shorter description of N7OM, auxiliary coefficients should be calculated with (1)-(7) [1]:

$$L_{AD} = L_d - l_d \tag{1}$$

$$L_{AQ} = L_q - l_q \tag{2}$$

$$l_F = L_{AD}\frac{L_d' - l_d}{L_d - L_d'} \tag{3}$$

$$l_D = \frac{L_{AD} l_F (L_d'' - l_d)}{L_{AD} l_F - (l_F + L_{AD})(L_d'' - l_d)} \tag{4}$$

$$l_Q = L_{AQ}\frac{L_d'' - l_d}{L_q - L_d''} \tag{5}$$

$$\frac{1}{L_{MD}} = \frac{1}{L_{AD}} + \frac{1}{l_d} + \frac{1}{l_F} + \frac{1}{l_D} \tag{6}$$

$$\frac{1}{L_{MQ}} = \frac{1}{L_{AQ}} + \frac{1}{l_q} + \frac{1}{l_Q} \tag{7}$$

The N7OM is now described by sets of algebraic equations (8)–(17) [1]:

$$\lambda_{AD}(t) = L_{MD}\left(\frac{\lambda_d(t)}{l_d} + \frac{\lambda_F(t)}{l_F} + \frac{\lambda_D(t)}{l_D}\right) \tag{8}$$

$$\lambda_{AQ}(t) = L_{MQ}\left(\frac{\lambda_q(t)}{l_q} + \frac{\lambda_Q(t)}{l_Q}\right) \tag{9}$$

$$i_d(t) = \frac{1}{l_d}\left(\lambda_d(t) - \lambda_{AD}(t)\right) \tag{10}$$

$$i_q(t) = \frac{1}{l_q}\left(\lambda_q(t) - \lambda_{AQ}(t)\right) \tag{11}$$

$$i_{\mathrm{F}}(t)=\frac{1}{l_{\mathrm{F}}}\left(\lambda_{\mathrm{F}}(t)-\lambda_{\mathrm{AD}}(t)\right) \quad (12)$$

$$i_{\mathrm{D}}(t)=\frac{1}{l_{\mathrm{D}}}\left(\lambda_{\mathrm{D}}(t)-\lambda_{\mathrm{AD}}(t)\right) \quad (13)$$

$$i_{\mathrm{Q}}(t)=\frac{1}{l_{\mathrm{Q}}}\left(\lambda_{\mathrm{Q}}(t)-\lambda_{\mathrm{AQ}}(t)\right) \quad (14)$$

$$v_{\mathrm{d}}(t)=-\sqrt{3}V_{\infty}\sin\left(\delta(t)\right)+R_{\mathrm{e}}i_{\mathrm{d}}(t)+\omega(t)L_{\mathrm{e}}i_{\mathrm{q}}(t) \quad (15)$$

$$v_{\mathrm{q}}(t)=\sqrt{3}V_{\infty}\cos\left(\delta(t)\right)+R_{\mathrm{e}}i_{\mathrm{q}}(t)+\omega(t)L_{\mathrm{e}}i_{\mathrm{d}}(t) \quad (16)$$

$$T_{\mathrm{e}}(t)=\frac{1}{3}\left(i_{\mathrm{q}}(t)\lambda_{\mathrm{d}}(t)-i_{\mathrm{d}}(t)\lambda_{\mathrm{q}}(t)\right) \quad (17)$$

and differential equations (18)-(24) [1]:

$$\dot{\lambda}_{\mathrm{d}}(t)=\omega_{\mathrm{s}}\left(-R_{\mathrm{s}}i_{\mathrm{d}}(t)-\omega(t)\lambda_{\mathrm{q}}(t)-v_{\mathrm{d}}(t)\right) \quad (18)$$

$$\dot{\lambda}_{\mathrm{q}}(t)=\omega_{\mathrm{s}}\left(-R_{\mathrm{s}}i_{\mathrm{q}}(t)+\omega(t)\lambda_{\mathrm{d}}(t)-v_{\mathrm{q}}(t)\right) \quad (19)$$

$$\dot{\lambda}_{\mathrm{F}}(t)=\omega_{\mathrm{s}}\left(-R_{\mathrm{F}}i_{\mathrm{F}}(t)+v_{\mathrm{F}}(t)\right) \quad (20)$$

$$\dot{\lambda}_{\mathrm{D}}(t)=\omega_{\mathrm{s}}\left(-R_{\mathrm{D}}i_{\mathrm{D}}(t)\right) \quad (21)$$

$$\dot{\lambda}_{\mathrm{Q}}(t)=\omega_{\mathrm{s}}\left(-R_{\mathrm{Q}}i_{\mathrm{Q}}(t)\right) \quad (22)$$

$$\dot{\omega}(t)=\frac{1}{2H}\left(T_{\mathrm{m}}(t)-T_{\mathrm{e}}(t)\right) \quad (23)$$

$$\dot{\delta}(t)=\omega_{\mathrm{s}}\left(\omega(t)-1\right) \quad (24)$$

where $i_{\mathrm{d}}(t)$ and $i_{\mathrm{q}}(t)$ are the stator d- and q-axis currents, $i_{\mathrm{F}}(t)$ is field current, $i_{\mathrm{D}}(t)$ and $i_{\mathrm{Q}}(t)$ are damping d- and q-axis currents, $v_{\mathrm{d}}(t)$ and $v_{\mathrm{q}}(t)$ are stator terminal d- and q-axis voltages, $\lambda_{\mathrm{AD}}(t)$ and $\lambda_{\mathrm{AQ}}(t)$ are d- and q-axis mutual flux linkages and $T_{\mathrm{e}}(t)$ is an electromagnetic torque. All variables in (2), (3) are normalized on the base quantities from Table II except mechanical torque $T_{\mathrm{m}}(t)$ and electric torque $T_{\mathrm{e}}(t)$, which are normalized on three-phase power base $S_{\mathrm{base,3p}}=3\,S_{\mathrm{base,1p}}$ and mechanical speed $\omega(t)$, respectively. The speed is normalized on base value $\omega_{\mathrm{mbase}}=\omega_{\mathrm{s}}/p$, where p is a number of pole pairs. In this way, dimensional mechanical speed can be directly calculated from normalized mechanical speed. Electric rotor angle $\delta(t)$ has unit [rad].

III. Linearized 3-rd Order Model of SG

Main disadvantage of N7OM is its un-suitability for an analytical dynamic analysis and control system design. Additional weakness of N7OM represents difficult tests for measurement and calculation of the SG's data. This is the reason that many simplified models of SG can be found in [1]-[3]. Their simplification is made up by neglecting some less important electromechanical phenomena. In such a way, linearized reduced order models of SG are established. Among many linearized reduced orders models, L3OM is the most popular. For development of this model, following assumptions are made [1]:

- balanced conditions are assumed and saturation effects are neglected,
- stator winding resistance is neglected,
- damping phenomena are neglected,
- $\dot{\lambda}_{\mathrm{d}}(t)$ and $\dot{\lambda}_{\mathrm{q}}(t)$ terms in stator equations are neglected and compared against speed voltage terms $\omega(t)\,\lambda_{\mathrm{d}}(t)$ and $\omega(t)\,\lambda_{\mathrm{q}}(t)$,
- terms $\omega(t)\,\lambda_{\mathrm{d}}(t)$ in stator and voltage equation are assumed to be approximately equal to $\omega_{\mathrm{s}}(t)\,\lambda_{\mathrm{d}}(t)$

Under the assumptions above, L3OM is obtained from N7OM by means of linearization for an every steady-state operating point (i. e. an equilibrium point). The L3OM describes the SG's dynamics in proximity of the selected equilibrium point. The L3OM has two inputs and three state-space variables. The inputs are mechanical torque $T_{\mathrm{m}\Delta}(t)$ and rotor excitation winding voltage $v_{\mathrm{f}\Delta}(t)$ deviations, the state-space variables are rotor angle $\delta_{\Delta}(t)$, rotor speed $\omega_{\Delta}(t)$ and voltage behind transient reactance $e'_{\mathrm{q}\Delta}(t)$ deviations. Additional outputs are electric torque $T_{\mathrm{e}\Delta}(t)$ and terminal stator voltage $v_{\mathrm{t}\Delta}(t)$ deviations. All the inputs and the state- space variables denote the deviations (subscript Δ) from the equilibrium state. The minimum set of the parameters and the steady-state variables of: SG, the transmission line and the infinite bus, necessary to calculate the coefficients of L3OM are presented in Table IV.

TABLE IV
SG'S DATA FOR L3OM

Parameters of SG	L_{d} [H], L_{q} [H], L_{d}' [H], H [s], R_{e} [Ω], L_{e} [H], D [pu], T'_{d0} [s]
Steady-state quantities of SG	P [W], Q [VAr], ω_{s} [rad s^{-1}], V_{∞} [V]

New parameters in Table IV are: D is a damping coefficient representing total lumped damping effects and T'_{d0} is an open circuit time constant of a direct axis.

From the data in Table IV, the equilibrium state for L3OM is calculated by means of a phasor diagram. Steady-state values in Table V must be determined before the calculation of the L3OM coefficients.

TABLE V
AUXILIARY STEADY-STATE VARIABLES FROM PHASOR DIAGRAM FOR L3OM

auxiliary steady-state variables for L3OM coefficients	δ_{ss}, $v_{\mathrm{d,ss}}$, $v_{\mathrm{q,ss}}$, $i_{\mathrm{d,ss}}$, $_{\mathrm{iq,ss}}$, E_{ss}, $E'_{\mathrm{q,ss}}$, $E_{\mathrm{qa,ss}}$

Index $_{\mathrm{ss}}$ means a steady-state value, while E, E_{qa} and E'_{q} are standardized phasor diagram EMF.

From the values in Tables IV and V, linearization coefficients K_1 to K_6 of L3OM are calculated [1].

The inputs, the state-space variables and the coefficients of L3OM are collected in Table VI.

TABLE VI
L3OM'S INPUTS, STATE-SPACE VARIABLES AND COEFFICIENTS

Inputs of L3OM	$T_{m\Delta}(t)$, $v_{f\Delta}(t)$
State-space variables of L3OM	$\omega_\Delta(t)$, $\delta_\Delta(t)$, $e'_{q\Delta}(t)$
Coefficients of L3OM	K_1, K_2, K_3, K_4, K_5, K_6, T'_{d0}, H, D

The L3OM is presented in a state-space form by (25) and (26):

$$\begin{bmatrix} \dot{\delta}_\Delta(t) \\ \dot{\omega}_\Delta(t) \\ \dot{e}'_{q\Delta}(t) \end{bmatrix} = \begin{bmatrix} 0 & \omega_r & 0 \\ -\frac{K_1}{2H} & -\frac{D}{2H} & -\frac{K_2}{2H} \\ -\frac{K_4}{T'_{d0}} & 0 & -\frac{1}{K_3 T'_{d0}} \end{bmatrix} \begin{bmatrix} \delta_\Delta(t) \\ \omega_\Delta(t) \\ e'_{q\Delta}(t) \end{bmatrix} + \begin{bmatrix} 0 & 0 \\ \frac{1}{2H} & 0 \\ 0 & \frac{1}{T'_{d0}} \end{bmatrix} \begin{bmatrix} T_{m\Delta}(t) \\ v_{f\Delta}(t) \end{bmatrix} \quad (25)$$

$$\begin{bmatrix} T_{e\Delta}(t) \\ v_{t\Delta}(t) \end{bmatrix} = \begin{bmatrix} K_1 & 0 & K_2 \\ K_5 & 0 & K_6 \end{bmatrix} \begin{bmatrix} \delta_\Delta(t) \\ \omega_\Delta(t) \\ e'_{q\Delta}(t) \end{bmatrix} + \begin{bmatrix} 0 & 0 \\ 0 & 0 \end{bmatrix} \begin{bmatrix} T_{m\Delta}(t) \\ v_{f\Delta}(t) \end{bmatrix} \quad (26)$$

All parameters and variables in L3OM are normalized except electric rotor angle $\delta(t)$.

IV. EXPERIMENTAL AND SIMULATION RESULTS

To evaluate the suitability and accuracy of the models, salient-pole SG with nominal power 15 kVA was used. Manufacturer's data are shown in Table VII.

TABLE VII
MANUFACTURERS' DATA OF TESTED SG

P_n=12 [kW]	U_n=400 [V]	I_n=21.7 [A]	cos φ_n=0.8
U_{Fn}=400 [V]	I_{Fn}=21.7 [A]	f_n=50 [Hz]	n_n=1500 [min^{-1}]

The P_n denotes rated active power, U_n, I_n, U_{Fn}, I_{Fn} are rated stator and excitation winding voltages and currents, respectively. The f_n and n_n are rated frequency and mechanical speed, respectively.

To determine the SG's parameters, a wide range of testing methods was devised [7]. In a frame of presented work, the standardized steady-state, transient and frequency-response tests were used [8], [9]. Obtained SG's parameters are shown in Table VIII.

TABLE VIII
SG'S DATA OBTAINED WITH TESTS

L_d=2.11 [pu]	L_q=1.45 [pu]	L_d'=0.25 [pu]	L_d''=0.18 [pu]
l_d=0.15 [pu]	l_q=0.15 [pu]	R_s=0.05 [pu]	R_F=0.015 [pu]
R_D=0.262 [pu]	R_Q=1.08 [pu]	R_e=0.003 [pu]	L_e=0.03 [pu]
H=0.19 [pu]	D=1 [pu]	T'_{d0}=0.5 [s]	ω_s=2π50 [s^{-1}]

For a nominal operating point, the calculated linearization coefficients are given in Table IX.

The testing system for determination of the parameter and experiments is shown in Fig. 1.

TABLE IX
LINEARIZATION PARAMETERS OF L3OM FOR NOMINAL OPERATING POINT
S_N=15 KVA, COS Φ_N=0.8

P_n=0.8 [pu]	K_1=2.1555	K_2=2.0815	K_3=0.1285
Q_n=0.6 [pu]	K_4=3.5155	K_5=0.0228	K_6=0.0998

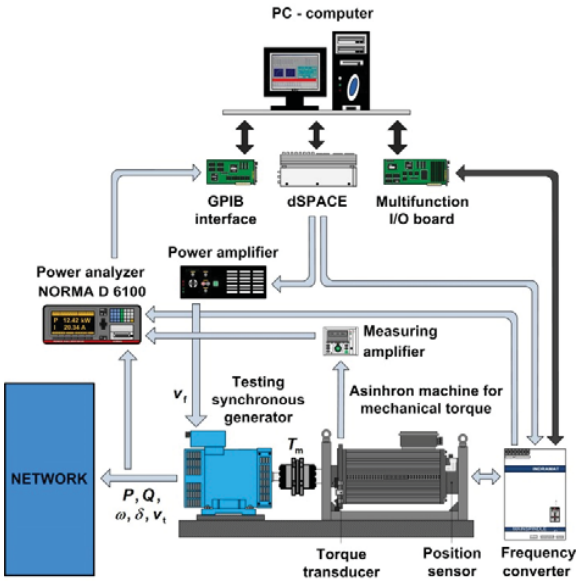

Fig. 1 Testing system

Fig. 2 shows the experimental and corresponding N7OM's simulation results. The curves on Fig. 2 (a) show the rotor speed responses to a 5% step change of the mechanical torque from the nominal operating point (i.e. from T_m = 0.8 [pu] to T_m = 0.84 [pu] in t = 0.5 [s]). The curves on Fig. 2 (b) show rotor speed responses to a 5 % step change of field excitation voltage from the nominal operating point (i.e. from v_f = 2.8 [pu] to v_f = 2.94 [pu] in t = 0.5 [s]). It is evident from Fig. 2 that N7OM well describes responses of real SG to the changes in the both inputs. Agreement in the first amplitude, the frequency and the damping of the transient response is very high. The experiments and the N7OM simulations were carried out in many operating points in the entire operating range of SG. In the entire range, N7OM represents accurate description of the dynamics of real SG.

To evaluate accuracy of the L3OM, simulations of N7OM and L3OM with same inputs and initial conditions were carried out and compared. Fig. 3 shows the rotor speed, rotor angle and terminal stator voltage responses to a 5% step change of the mechanical torque from the nominal operating point (i.e. from T_m = 0.8 [pu] to T_m = 0.84 [pu] in t = 0.5 [s]). Fig. 4 shows the rotor speed, rotor angle and terminal stator voltage responses to the 5% step change of the rotor excitation voltage from the nominal operating point (i.e. from v_f = 2.8 [pu] to v_f = 2.94 [pu] in t = 0.5 [s]). From both figures, the high accordance of L3OM is evident. To research suitability of L3OM in an entire operating range of SG (from P = 0 [pu] to P = 1.2 [pu] and from Q = -1.2 [pu] to Q = 1.2 [pu]), a systemic numerical analysis of the both models in the entire operating range was conducted. The conclusion is that L3OM

describes SG's electro mechanical phenomena in the entire operating range in the case of the small input's perturbations.

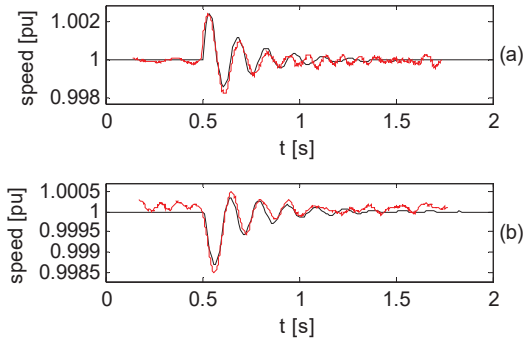

Fig. 2 Rotor speed response for step change of mechanical torque from $T_m = 0.8$ [pu] to $T_m = 0.84$ [pu] in $t = 0.5$ [s] (a) and step change of field excitation voltage from $v_f = 2.8$ [pu] to $v_f = 2.94$ [pu] in $t = 0.5$ [s] (b) obtained with experiment (more oscillating graph) and N7OM simulation (constant in steady state)

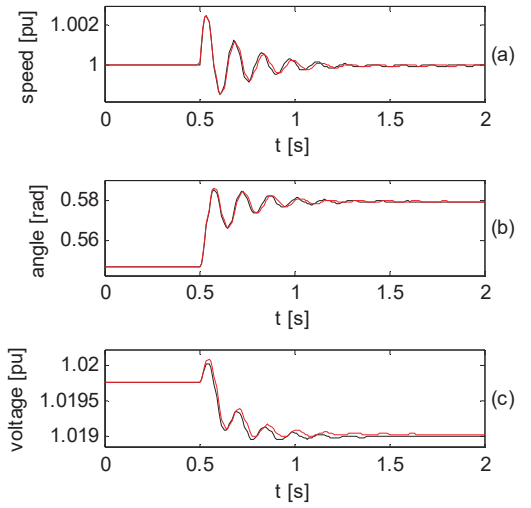

Fig. 3 Rotor speed (a), rotor angle (b) and terminal stator voltage (c) for step change of mechanical torque from $T_m = 0.8$ [pu] to $T_m = 0.84$ [pu] in $t = 0.5$ [s] obtained with N7OM simulation and L3OM simulation

V. Numerical Analysis of Dynamic Models

Main disadvantage of L3OM is its restriction to use only in "relative" proximity of the equilibrium state. An effect of larger input changes on discrepancy between responses obtained with N7OM and L3OM is shown in Figs. 5 and 6. Fig. 5 shows rotor speed, rotor angle and terminal stator voltage responses to a 50% step change of a mechanical torque from the nominal operating point (i.e. from $T_m = 0.8$ [pu] to $T_m = 1.2$ [pu] in $t = 0.5$ [s]). Fig. 6 shows the same variables' responses to the 50% step change of field excitation voltage from the nominal operating point (i.e. from $v_f = 2.8$ [pu] to $v_f = 4.2$ [pu] in $t = 0.5$ [s]). From both figures, larger inaccurateness of L3OM can be seen in the steady-state values and in the frequency and the damping of the transient responses.

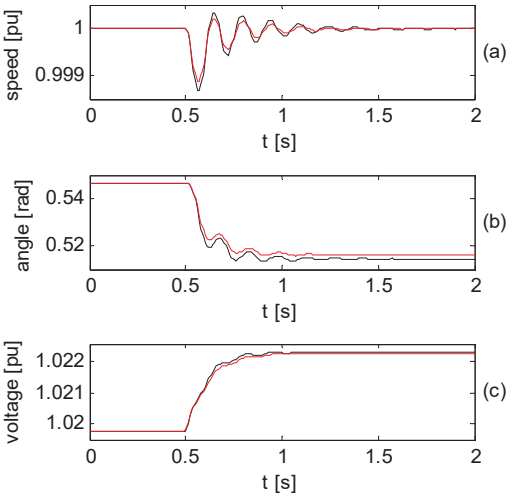

Fig. 4 Rotor speed (a), rotor angle (b) and terminal stator voltage (c) for step change of field excitation voltage from $v_f = 2.8$ [pu] to $v_f = 2.94$ [pu] in $t = 0.5$ [s] obtained with N7OM simulation and L3OM simulation

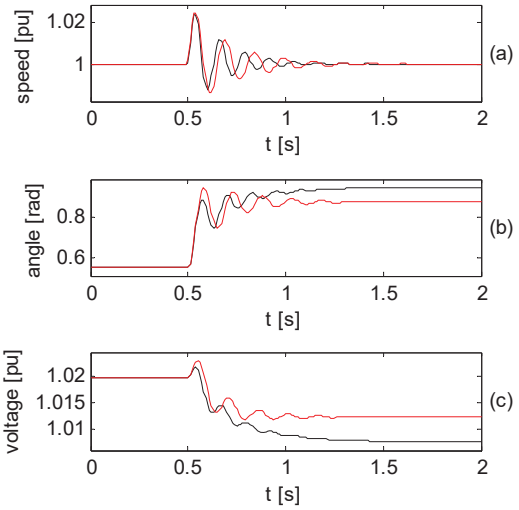

Fig. 5 Rotor speed (a), rotor angle (b) and terminal stator voltage (c) for step change of mechanical torque from $T_m = 0.8$ [pu] to $T_m = 1.2$ [pu] in $t = 0.5$ [s] obtained with N7OM simulation (higher steady state in 5 (b) and lower steady state in 5 (c)) and L3OM simulation

Limits of the equilibrium state, where L3OM is accurate enough to replace N7OM are estimated with the systemic numerical analysis. It is carried out in the entire operating range for various inputs. The evaluation of the steady-state accuracy and the dynamic quality of L3OM is made.

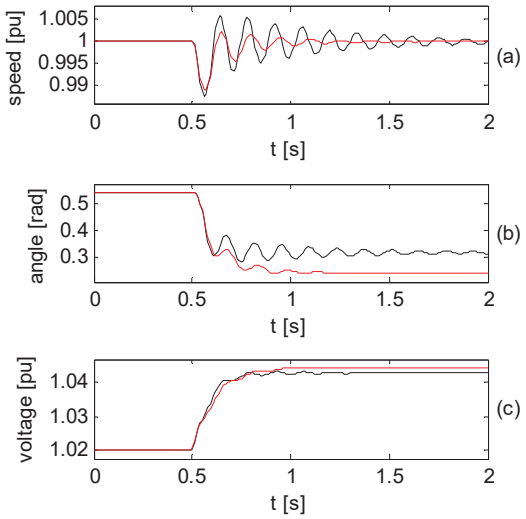

Fig. 6 Rotor speed (a), rotor angle (b) and terminal stator voltage (c) for step change of the field excitation voltage from $v_f = 2.8$ [pu] to $v_f = 4.2$ [pu] in $t = 0.5$ [s] obtained with N7OM simulation (more oscillating graph) and L3OM simulation

Fig. 7 shows the influence of mechanical torque deviations on a rotor angle error and on a stator voltage error between N7OM and L3OM in steady-states for a mechanical torque range from $T_{m\Delta} = -0.5$ [pu] to $T_{m\Delta} = +0.5$ [pu] around a nominal value of the torque. Figure 8 shows influence of field excitation voltage deviations on the rotor angle error and stator voltage error between the N7OM and L3OM in steady-states for deviation of field excitation voltage from $v_{f\Delta} = -1.0$ [pu] to $v_{f\Delta} = +1.0$ [pu] around the nominal value of the field excitation voltage. By means of diagrams in Figs. 7 and 8 we can estimate the steady-state errors of L3OM. It is also evident that the steady-state error characteristics are not symmetrical. Increase of the mechanical torque causes a larger steady-state error than its decrease. Increase of the field excitation voltage causes a smaller steady-state error than its decrease. This could be meaningful by selecting the corresponding equilibrium point for the investigated operating range.

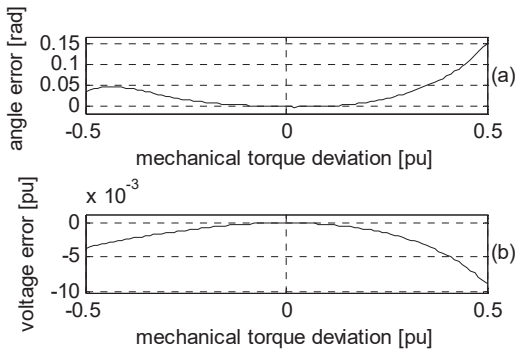

Fig. 7 Rotor angle error (a) and stator voltage error (b) between N7OM and L3OM steady-states for deviation of mechanical torque from $T_{m\Delta} = -0.5$ [pu] to $T_{m\Delta} = +0.5$ [pu] around nominal value of mechanical torque

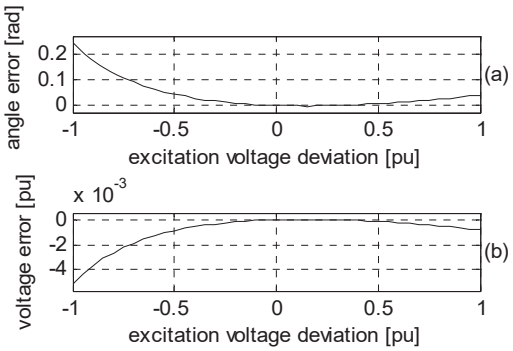

Fig. 8 Rotor angle error (a) and stator voltage error (b) between N7OM and L3OM steady states for deviation of field excitation voltage from $v_{f\Delta} = -1.0$ [pu] to $v_{f\Delta} = +1.0$ [pu] around nominal value of field excitation voltage

To research influence of the inputs' deviations on the dynamic accuracy of L3OM, an integral squared error between the speed responses of N7OM and L3OM during the transient states was introduced:

$$\mathrm{ISE} = \int (\omega_{\mathrm{N7OM}}(t) - \omega_{\mathrm{L3OM}}(t))^2 \, \mathrm{d}t \tag{27}$$

where $\omega_{\mathrm{N7OM}}(t)$ and $\omega_{\mathrm{L3OM}}(t)$ denote the rotor electric speed of N7OM and L3OM, respectively during the transient states. Fig. 9 shows a square root of an integral squared error as a function of mechanical torque deviation from $T_{m\Delta} = -0.5$ [pu] to $T_{m\Delta} = +0.5$ [pu] around the nominal value and as a function of field excitation voltage from $v_{f\Delta} = -1.0$ [pu] to $v_{f\Delta} = +1.0$ [pu] around the nominal value.

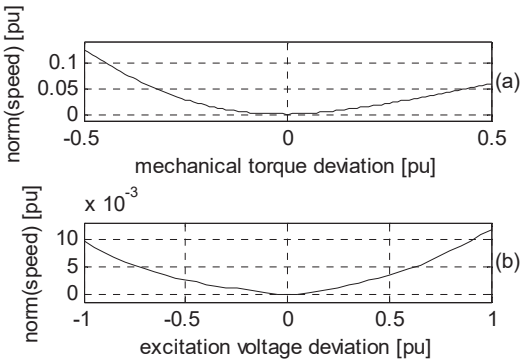

Fig. 9 Square root of integral squared error ("norm(speed)") between rotor speed transients of N7OM and L3OM for step changes of mechanical torque from $T_{m\Delta} = -0.5$ [pu] to $T_{m\Delta} = +0.5$ [pu] from nominal value of mechanical torque (a) and step changes of field excitation voltage from $v_{f\Delta} = -1.0$ [pu] to $v_{f\Delta} = +1.0$ [pu] from nominal value of field excitation voltage (b)

A detailed systemic numerical analysis was conducted for different SG in the entire operating range. Obtained error functions have a same form and very similar values as functions on Figs. 7-9 in the entire region.

VI. Comparison of N7OM and L3OM

Applicability with feasibility and accuracy of the studied SG's models was evaluated for representative scenarios as objectively as possible. The evaluation is based on the systemic numerical calculations for hydro- and turbo-generators of different power in the entire operating range for different inputs deviations and initial conditions. For a purpose of catalogue data of analysed generators, additional data are calculated. The data are calculated with N7OM for each generator and with appropriate L3OMs for each generator at different operating points. The data of generators are obtained from [1] and documentation of Slovenian power plants. In this way, qualitative estimates of usability of L3OM in different categories are obtained.

On a basis of the theoretical analysis, the numerical simulations and the laboratory experiments, the quality grades for the both models were established. An associate scale consists of the seven grades marked from "---" to "+++". The following ten investigated categories were evaluated:

- accuracy in small operating range around steady-state,
- accuracy in entire operating range,
- complexity of models' structure (order, non-linearities),
- number of SG's data for models' parameters calculation
- obtained models' output variables,
- suitability of models for numerical simulations (computing demand, integration step size and integration method),
- suitability of models for theoretical analysis,
- suitability of models for eigenvalue analysis,
- suitability of models for control system design and synthesis,
- possibility to comprehend saturation phenomena.

Evaluation of proposed L3OM for all the investigated categories is presented in Table X.

TABLE X
Assessment of Studied Models

sphere of activity	N7OM	L3OM
accuracy in small range	+++	+++
accuracy in entire range	+++	-
complexity	--	+++
necessary SG's data	---	+
obtained output variables	+++	+
numerical simulations	+	+++
theoretical analysis	--	+++
eigenvalue analysis	---	+++
control design and synthesis	--	+++
saturation phenomena	++	---

VII. Summary with Conclusions

The main contribution of the paper is theoretical and laboratory experimental study of certain characteristics of L3OM and its applicability and accuracy in selected scenarios. On the basis of the defined characteristics, the steady-state and dynamic integral squared errors can be estimated within the theoretical and numerical evaluation. They mainly arise as consequences of the simplification and linearization of the basic full order non-linear model. The presented results improve knowledge for improved decisions regarding design, synthesis and testing of the SG's control systems (e. g. power system stabilizers).

The secondary contribution of the paper is the unified presentation with direct comparison of the complex backgrounds, advantages and disadvantages of existing N7OM and L3OM. This consideration includes complexity, electromagnetic and electromechanical characteristics, state restrictedness and adaptiveness, and accessibility in operation. The inferred knowledge offers auxiliary support and convenience to professionals for selecting the appropriate model in the considered operating conditions.

References

[1] P. M. Anderson and A. A. Fouad, *Power System Control and Stability*. The Iowa State University Press, Ames, Iowa. 1977.
[2] P. Kundur, *Power System Stability and Control*. McGraw-Hill, Inc., New York, 1994.
[3] I. Boldea, *Synchronous Generators*. Taylor & Francis Group, Boca Raton, 2016.
[4] W. G. Heffron and R. A. Phillips, "Effect of a Modern Amplidyne Voltage Regulator on Underexcited Operation of Large Turbine Generators", *AIEE Transactions*, vol. 71, pp. 692-697, 1952.
[5] M. Soliman, D. Westwick and O. P. Malik, "Identification of Heffron-Phillips model parameters for synchronous generators operating in closed loop", *IET Generation, Transmission & Distribution,* vol.2, no.4, pp. 530-241, 2008.
[6] C. M. S. Neto, F. B. Costa, R. L. A. Ribeiro, R. L. Barreto and T. O. A. Rocha, "Wavelet-Based Power System Stabilizer", *IEEE Transactions on Industrial Electronics,* vol.62, no.12, pp. 7360-7369, 2015.
[7] M. Karrari and O. P. Malik, "Identification of physical parameters of a synchronous generator from online measurement", *IEEE Trans. on Energy Conversion,* vol.19, no.2, pp. 407-415, 2004.
[8] *IEEE Guide for Synchronous Generator Modeling - Practices and Applications in Power System Stability Analyses,* IEEE Standard 1110, 2002.
[9] *Rotating Electrical Machines – Methods for Determining Synchronous Machine Quantitites from Tests,* IEC Standard 60034-4, 2008